RSC Sustainability

ROYAL SOCIETY OF CHEMISTRY

PAPER

View Article Online
View Journal | View Issue

Cite this: *RSC Sustainability*, 2025, **3**, 1494

Optimizing nanoparticle-mediated drug delivery: insights from compartmental modeling *via* the CompSafeNano cloud platform

Periklis Tsiros,[a] Nikolaos Chimarios,[b] Dimitrios Zouraris,[bc] Andreas Tsoumanis,[bc] Haralambos Sarimveis,[a] Georgia Melagraki,[d] Iseult Lynch[e] and Antreas Afantitis *[bc]

The deployment of nanoparticles (NPs) for targeted drug delivery *in vivo* holds immense potential for enhancing therapeutic efficacy while minimizing systemic side effects. However, the complexity of biological environments, including the biological barriers that need to be crossed for effective systemic delivery, presents significant challenges in optimizing NP delivery. This study demonstrates how a simple compartmental model facilitates the simulation and analysis of NP-mediated drug delivery, supporting targeted delivery optimization. The model involves reversible transport between five compartments related to drug delivery (administration site, off-target sites, target cell vicinity, target cell interior and excreta) that determine NP dynamics, including biodistribution, degradation, and excretion processes. This approach enables the estimation of delivery efficiency and the identification of critical factors affecting NP delivery through sensitivity analysis. A case study involving PEG-coated gold NPs delivered intravenously to the lungs demonstrates the model's capacity to describe observed biodistribution patterns and highlights key parameters influencing delivery outcomes. The model is exposed as a web application that provides a user-friendly graphical interface, enabling researchers to conduct *in silico* experiments with the goal of optimizing delivery strategies, thereby accelerating the development of precision nanomedicine. The model is made available both as a web application, *via* the Enalos Cloud Platform, and as a RESTful aaplication programming interface (API), providing a user-friendly graphical interface and programmatic access, respectively, enabling researchers to integrate the model into their own computational workflows. This study illustrates how simple compartmental modelling can be employed to guide the development of targeted drug delivery systems, contributing to more effective and personalized healthcare interventions.

Received 6th November 2024
Accepted 26th January 2025

DOI: 10.1039/d4su00686k

rsc.li/rscsus

Sustainability spotlight

This work advances sustainability by introducing a computational tool that optimizes nanoparticle-mediated drug delivery, reducing reliance on extensive *in vivo* experimentation and thereby minimizing resource consumption and ethical concerns associated with animal testing. By enhancing the efficiency of targeted drug delivery, it contributes to UN Sustainable Development Goal (SDG) 3: good health and well-being, promoting more effective and personalized medical treatments. The model's potential extension to precision agriculture aligns with SDG 2: zero hunger, by improving nutrient and agrichemical delivery to crops, enhancing yields while reducing environmental impact. Additionally, the web application's democratization of advanced modeling tools fosters innovation (SDG 9: industry, innovation, and infrastructure) and supports responsible consumption and production (SDG 12) through efficient resource use in nanomedicine development.

1. Introduction

The field of nanoparticle (NP) based drug delivery has witnessed rapid advances, offering promising solutions for targeted and efficient therapeutic and theranostic interventions.[1] Targeted drug delivery represents a transformative approach in modern medicine, aiming to direct therapeutic agents precisely to the diseased site while minimizing systemic exposure and side effects resulting from accumulation of the therapeutic agent

[a]*School of Chemical Engineering, National Technical University of Athens, Athens, Greece*
[b]*NovaMechanics Ltd, Nicosia, Cyprus. E-mail: afantitis@novamechanics.com*
[c]*Entelos Institute, Larnaca 6059, Cyprus*
[d]*Division of Physical Sciences and Applications, Hellenic Military Academy, Vari 16672, Greece*
[e]*School of Geography, Earth and Environmental Sciences, University of Birmingham, Birmingham, UK*

away from the site of action, or off-site. Targeting strategies are thus designed to enhance treatment efficacy and reduce adverse effects, particularly in oncology, where precision is paramount.[2–4] The field of NP-mediated delivery has emerged as a promising avenue for achieving targeted drug delivery, leveraging the unique properties of NPs to navigate the complex biological environment and deliver drugs efficiently to specific cellular targets.[5] NP delivery, however, presents a complex interplay of physiological, pharmacological, and biophysical factors that challenge the accurate prediction and optimization of drug delivery outcomes, and hinders transfer of nano-based medicines from lab to clinical practice.[6]

NP-mediated drug delivery offers several distinct advantages over conventional drug delivery systems. Engineered NPs (ENPs) can significantly enhance drug solubility, stability, and bioavailability, leading to improved pharmacokinetic profiles and therapeutic outcomes.[7,8] The nanoscale dimensions, surface properties, and functionalization potential of NPs allow for the attachment of specific targeting ligands, which facilitate precise binding to pathological cells.[5] This targeted delivery minimizes off-target effects and elevates the therapeutic index of the drugs administered, which is the ratio between the dose required to produce an adverse effect (*e.g.*, LD_{50}, TD_{50} *etc.*) and the dose necessary to achieve therapeutic effects. However, the application of NP-mediated delivery involves several complexities. The heterogeneous and dynamic nature of *in vivo* environments necessitates that NPs navigate and surmount a series of biological barriers, which depend on the administration route and target site. These barriers can include the air-lung barrier, the blood–brain barrier as well as cellular membranes. To reach specific tissues, NPs must also avoid clearance by the reticuloendothelial system (RES), ensure immune system evasion, and access efficient cellular internalization.[9–11] Moreover, the potential cytotoxicity and the long-term biodistribution and biocompatibility of NPs are critical factors that require comprehensive investigation and continuous monitoring.[12,13]

NP delivery *in vivo* involves a complex interplay of physiological, pharmacological, and biophysical parameters; optimizing NP-mediated drug delivery necessitates a comprehensive understanding of these factors and their influence on NP biodistribution and therapeutic efficacy. Traditional biokinetics modeling methodologies to explain the biodistribution of medicines, such as physiologically-based kinetic (PBK) models, offer detailed insights into the rates of uptake and clearance of therapeutic agents but require extensive input data and computational resources.[8,14] Alternatively, compartmental models provide a simplified framework, typically consisting of a few abstract compartments, such as central and peripheral compartments, with rate constants describing the translocation of substances between them.[15] Parameters in these models are estimated using a top-down approach, fitting the model directly to available *in vivo* data. This streamlined structure makes compartmental models easier to parameterize and suitable for cases where detailed physiological data are not available. The lack of mechanistic detail and direct physiological relevance of compartments limits the applicability of compartmental models, particularly in their ability to extrapolate across different systems, such as different doses, species, life stages, administration routes, or disease states. This limitation reduces their utility for predicting NP behavior *in vivo* under untested conditions. Nevertheless, these models can provide valuable insights into how biological barriers influence NP delivery and help identify kinetic bottlenecks. Sensitivity analysis, in particular, can highlight key biological processes – implicitly represented in the translocation rates – that significantly impact delivery efficiency. These insights can inform strategies to optimize NP delivery to target cells through a functional-by-design approach, analogous to the well-established safe-by-design strategy.

Here we present the implementation of a compartmental model as a tool to guide the design process for optimizing NP drug delivery efficacy. The mathematical framework for the quantitative description of *in vivo* NP delivery processes is presented *via* a user-friendly graphical web application enabling its widespread utilization. The core idea of the model is that targeted delivery efficiency can be analyzed *in silico* by considering just a few relevant sites (compartments) that reflect the core locations involved in the delivery process including the administration site, off-target sites, target cell vicinity and target cell interior.[16] The delivery efficiency can be dynamically expressed through the model as the ratio of the quantity of NPs reaching the target cell interior relative to the total administered dose.

2. Methodology

2.1. Compartmental modelling for NP delivery optimization

In a recent publication,[16] a simple compartmental model was proposed, which includes just a few critical compartments, namely the administration site, off-target sites, target cell vicinity and the target cell interior. The administration site represents the entry port to the body and, naturally, varies depending on the administration route, with the most common sites being the blood, gut and lungs, following intravenous injection, oral administration and inhalation, respectively. Once in the body, NPs can move from the administration site to the vicinity of the target cell, *via* translocation across different cell layers and tissue stroma. The target cell vicinity can be viewed as the interstitial space that is in direct contact with the target cells. Alternatively, NPs can be translocated from the administration site to off-target sites, *i.e.*, different cell types or tissues other than the target. In addition, NPs can move from the target cell vicinity to off-target sites through various clearance mechanisms, *e.g.*, through lymphatic drainage or phagocytosis. Finally, after reaching the target cell's vicinity, NPs can be taken up (internalized) by the target cells through endocytosis.[10] The reader is referred to ref. 16 for a comprehensive review of the different biological processes that affect the presented translocation rates between each of these compartments.

In this study performed as part of the CompSafeNano project to develop *in silico* tools for NPs safety and efficacy assessment, the model of ref. 16 was extended to facilitate *in silico*

simulation of the biodistribution patterns of NPs. In particular, each transport process presented in the original model was considered to be irreversible. However, most biological transport phenomena are reversible. As a result, all transport rates are regarded as reversible in this study. The inclusion of an additional translocation from the vicinity of the target cell back to the administration site is particularly warranted, especially when the administration route involves intravenous injection and thus systemic circulation. This rationale stems from the perfusion of all tissues by arterial blood, which subsequently converges into the venous blood pool. Venous blood then passes through the lungs, where it is enriched with oxygen, and reaches all tissues again as arterial blood. In addition to the blood loop, many chemicals are removed from a tissue *via* lymph drainage. Chemicals that are removed through this pathway can re-enter blood from the right lymphatic duct and thoracic duct, where lymph rejoins the bloodstream. Thus, this complex loop can effectively act as a chemical or NP recycling process. Therefore, this translocation pathway is significant in the context of optimizing delivery outcomes. The same reasoning can be applied for justifying a translocation rate from off-target sites back to the administration site. The movement of NPs from the target cell interior to the target cell vicinity is described by the process of exocytosis.[17] Likewise, the rate at which substances translocate from off-target sites back to the vicinity of the target cell encompasses various processes, including exocytosis originating from neighboring cells within the target cell vicinity area, but of a different cellular phenotype.

In pursuit of comprehensive refinement of the earlier model, apart from rendering all processes reversible, additional compartments and flows were integrated into the original compartmental model. Specifically, a compartment was included in order to describe the amount of NPs excreted from the body. NPs from both the administration site and the off-target tissues can end up in the excreta compartment. If the administration site is blood, then this flow of NPs can represent renal excretion, *i.e.*, renal filtration of arterial blood, while the translocation rate from off-target sites to excreta represents hepatobiliary elimination. If the target cell is hepatocytes, then an extra translocation rate from the cell interior to the off-target cells is considered, representing bile excretion from hepatocytes to the small intestine. The translocation of NPs to excreta is an irreversible process, in contrast to the rest of the translocation rates. Finally, each compartment supports a compartment-specific NP degradation rate, thus enabling simulation of biodegradable NPs. The extended model is schematically illustrated in Fig. 1.

The governing equations of the extended compartmental model are provided below, with the description of each of the variables provided in Table 1 below. Specifically, eqn (1) represents the rate of change of NP mass at the administration site due to transport to and from this location. Eqn (2)–(5) describe the respective rates of NP mass change in the cell vicinity, cell interior, off-target sites, and excreta. The total NP mass in the system is given by eqn (6), while eqn (7) is used to calculate delivery efficiency.

$$\frac{dNP_{AS}}{dt} = -\left(k_{AStCV} + k_{AStOT} + k_{AStEX} + k_{deg,AS}\right) \times NP_{AS} + k_{CVtAS} \times NP_{CV} + k_{OTtAS} \times NP_{OT} \quad (1)$$

$$\frac{dNP_{CV}}{dt} = -\left(k_{CVtAS} + k_{CVtCI} + k_{CVtOT} + k_{deg,CV}\right) \times NP_{CV} + k_{AStCV} \times NP_{AS} + k_{CItCV} \times NP_{CI} + k_{OTtCV} \times NP_{OT} \quad (2)$$

$$\frac{dNP_{CI}}{dt} = -\left(k_{CItCV} + k_{CItOT} + k_{deg,CI}\right) \times NP_{CI} + k_{CVtCI} \times NP_{CV} \quad (3)$$

$$\frac{dNP_{OT}}{dt} = -\left(k_{OTtAS} + k_{OTtCV} + k_{OTtEX} + k_{deg,OT}\right) \times NP_{OT} + k_{AStOT} \times NP_{AS} + k_{CVtOT} \times NP_{CV} + k_{CItOT} \times NP_{CI} \quad (4)$$

$$\frac{dNP_{EX}}{dt} = k_{AStEX} \times NP_{AS} + k_{OTtEX} \times NP_{OT} \quad (5)$$

$$NP_{TOT} = NP_{AS} + NP_{CV} + NP_{OT} + NP_{CI} + NP_{EX} \quad (6)$$

$$\text{Delivery efficiency} = \frac{NP_{CI}}{NP_{TOT}} \quad (7)$$

The biological processes that distribute NPs between these compartments are expressed *via* the rate constants of the ordinary differential equation (ODE) system. Note that the overall delivery efficiency is expressed as a ratio of two time-varying components, namely the NP mass in the cell interior relative to the total administered NP mass. Therefore, through eqn (7), the NP delivery efficiency can be analyzed in a time-resolved manner. A brief description of each parameter and state variable included in the extended compartmental model is provided in Table 1.

2.2. Demonstration case: targeted delivery of gold NPs to the lungs

The proposed generic ODE system aims to accelerate the optimization of NP delivery by identifying critical kinetic bottlenecks of the delivery process. To achieve this, the model should be parameterized for each case study consisting of a specific NP and target tissue cell combination, utilizing available biokinetic data. As a demonstration, we develop a model to analyze the delivery efficiency of gold NPs (Au NPs) with polyethylene glycol (PEG) coatings to the lungs *via* intravenous (IV) injection. Rather than employing a traditional top-down parameter estimation approach, we adopt a middle-out strategy, exploiting both *in vivo* and *in vitro* data for model parameterization. Specifically, *in vivo* data are utilized to estimate parameters describing the translocation of NPs in compartments other than the target cell, while *in vitro* data serve as the best-available proxies for estimating endocytosis and exocytosis rates of the target cell. The specific NP was selected for the demonstration

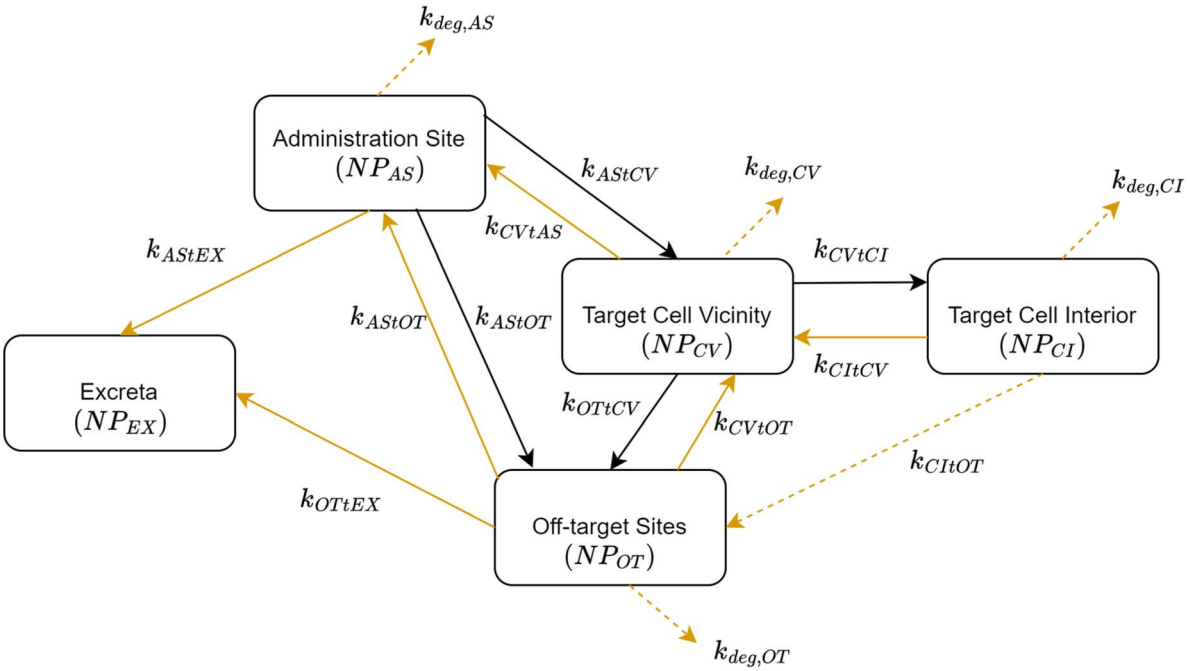

Fig. 1 Schematic representation of the proposed model for NP-mediated drug delivery. The model comprises an extension of the conceptual model proposed by Wu *et al.*,[18] with new translocation rates indicated by light orange. The dashed arrow from the target cell interior to off-target sites is relevant only when the target cells are hepatocytes, indicating bile flow. The rest of the dashed arrows signify NP degradation, which is applicable only to biodegradable NPs. For an explanation of the translocation rates, the reader is referred to Table 1.

because both *in vitro* and *in vivo* data related to PEG–Au NPs with the same physicochemical characteristics were available from the same research group, ensuring data consistency. To parameterize the model, we utilized the biodistribution data outlined in ref. 19, which provided comprehensive biokinetic details regarding the distribution of PEG–Au NPs following IV administration in rats. The PEG–Au NPs used in the study had a core size of 10.5 nm and a corresponding hydrodynamic size around 13 nm. The NPs were administered intravenously to male Wistar rats of initial weight around 220 g at a dose of 0.7 mg kg^{-1}, and tissue samples were collected at 1 h, 4 h, 24 h, 7 d and 28 d post injection. The authors focused on the primary physiological compartments that serve as reservoirs for NPs, and thus, the analysis included the kidneys, liver, spleen, lungs and blood.

The mass–time profiles for each organ reported in ref. 19 were transformed in order to facilitate parameter calibration of the compartmental model. Specifically, the data needed to be

Table 1 Description of model parameters and state variables used in the extended compartmental model of Fig. 1

Parameter	Description
k_{AStCV}	Translocation rate from administration site to target cell vicinity
k_{AStOT}	Translocation rate from administration site to off-target sites
k_{AStEX}	Translocation rate from administration site to excreta
k_{CVtAS}	Translocation rate from target cell vicinity to administration site
k_{CVtCI}	Translocation rate from target cell vicinity to cell interior
k_{CVtOT}	Translocation rate from target cell vicinity to off-target sites
k_{CItCV}	Translocation rate from target cell interior to target cell vicinity
k_{CItOT}	Translocation rate from target cell interior to off-target sites
k_{OTtAS}	Translocation rate from off-target sites to administration site
k_{OTtCV}	Translocation rate from off-target sites to target cell vicinity
k_{OTtEX}	Translocation rate from off-target sites to excreta
$k_{deg,i}$	NP degradation rate at compartment i
NP_{AS}	NP mass in administration site
NP_{CV}	NP mass in target cell vicinity
NP_{CI}	NP mass in target cell interior
NP_{OT}	NP mass in off-target sites
NP_{EX}	NP mass in excreta
NP_{TOT}	Total NP mass

mapped to the corresponding compartments of the model. The first step of the process involved identification of the target compartment. In this scenario, the lungs were selected as the target tissue for NP delivery, so the sum of NPs in the cell vicinity and cell interior was set equal to the NP mass in the lungs compartment during the parameter calibration process. The blood served as the site of administration since NPs were delivered to the target tissue *via* IV injection into the tail vein. Consequently, the rest of the organs, namely the liver, kidneys and spleen, were combined into the off-target sites compartment. The difference between the administered dose and the sum of dose per time point, as reported in ref. 19, was assigned to the excreta compartment, by assuming that tissues that were not included in the study accumulate a negligible amount of NPs. This assumption is supported by literature evidence, based on which, PEG–Au NPs are primarily translocated into the liver and spleen.[20] In addition to the biodistribution data that were utilized for parameter calibration, *in vitro* data were also incorporated into the model. Specifically,[21] exposed different cell lines to the same PEG–Au NPs used in ref. 19 and the internalized amounts allowed estimation of the NP cellular internalization and excretion rates. From the available human cell lines, the lung epithelial carcinoma (A549) was selected for its relevance to lung tissue. The cellular uptake (endocytosis) and excretion (exocytosis) rates from ref. 21 were directly used in our study to represent the translocation rates from the target cell vicinity to the target cell interior and *vice versa*.

The remaining parameters were estimated by fitting the model on the available biodistribution data. The Simulation-Observations Discrepancy Index (SODI) introduced in ref. 22 was employed as a goodness-of-fit metric for quantitatively comparing the experimental data with the curves produced by the ODE system. The methodology that facilitated the optimization process was the *Subplex* algorithm.[23] The optimization workflow was coded in the R programming language version 4.0.4. The system of ODEs was solved by employing the *lsodes* algorithm of the *deSolve* package.[24] Additionally, the Subplex method was integrated into the code through the *nloptr* package.[25]

3. Results

3.1. Parameter estimation and goodness-of-fit

The results of the parameter estimation and goodness-of-fit analysis are presented below. These findings provide a quantitative assessment of the model's ability to accurately describe the observed data and highlight the adequacy of the linear ODE system to accurately capture the NP dynamics as portrayed by the underlying biodistribution data. The best solution yielded a SODI metric equal to 0.88, which is equivalent to an absolute average fold error (AAFE) of 1.78. The parameter estimates of the model are presented in Table 2. Notably, the translocation rates from off-target sites to excreta and from off-target sites to the administration site were set to zero by the optimization algorithm. This implies that most NPs are excreted through renal clearance *via* glomerular filtration, *i.e.*, directly from arterial blood, which in this case is represented by the administration site, and not through hepatobiliary clearance, which in this model is represented through the translocation rate from off-target sites to excreta. The PEG–Au NPs used in this study have a core size of around 10 nm and a hydrodynamic size equal to 13 nm, which is close to the renal clearance filtration threshold that was found to be close to 10 nm in a previous study exploring renal clearance of quantum dots in mice,[26] and that is generally accepted.[27]

Table 2 Parameter values and units of the PEG–Au NPs case study after calibration of the extended compartmental model

Parameter	Value	Units	Source
k_{AStCV}	0.0178	h^{-1}	Calibrated using data from ref. 19
k_{AStOT}	0.0159	h^{-1}	Calibrated using data from ref. 19
k_{AStEX}	0.0758	h^{-1}	Calibrated using data from ref. 19
k_{CVtAS}	0.5688	h^{-1}	Calibrated using data from ref. 19
k_{CVtCI}	0.4000	h^{-1}	Based on ref. 21
k_{CVtOT}	1.5325	h^{-1}	Calibrated using data from ref. 19
k_{CItCV}	0.0598	h^{-1}	Based on ref. 21
k_{CItOT}	0.0000	h^{-1}	Not included in the model as this translocation rate specifically applies to hepatocytes, particularly the transport from hepatocytes to the small intestine *via* bile acids
k_{OTtAS}	0.0000	h^{-1}	Calibrated using data from ref. 19
k_{OTtCV}	0.0087	h^{-1}	Calibrated using data from ref. 19
k_{OTtEX}	0.0000	h^{-1}	Calibrated using data from ref. 19

The generated goodness-of-fit of the model on the experimental data is illustrated in Fig. 2. The extended compartmental model exhibited a satisfactory goodness-of-fit on the administration site, excreta, and cell vicinity & cell interior compartments. The latter compartment is the most crucial in terms of goodness-of-fit, as it directly defines and characterizes the target site and NP delivery efficiency, and any model deviations from the experimental data will also affect the downstream delivery efficiency *in silico* analysis. The model's predictive ability was somewhat less accurate for the off-target sites compartment, which nonetheless has little effect on the overall model assessment. The deviation of predictions from observations for the off-target sites compartment can be attributed to the simple, linear kinetics assumed by the model, in combination with the fact that the NP mass of the off-target sites compartment is an estimate derived through the summation of the measured tissues reported in ref. 19.

3.2. Sensitivity analysis

An important aspect of estimating NP delivery efficiency through compartmental modeling is the ability to perform dynamic sensitivity analysis. In particular, the amount of NPs entering and exiting the target site is not constant but is substantially influenced by the progress of other biodistribution processes, such as systemic clearance. Therefore, different kinetic profiles could result in different dynamic patterns in relation to the delivery efficiency, *e.g.*, a different maximum, a different time to reach maximum *etc.* Fig. 3 highlights the importance of conducting sensitivity analysis for evaluating the efficacy of NP delivery and further elucidating critical factors

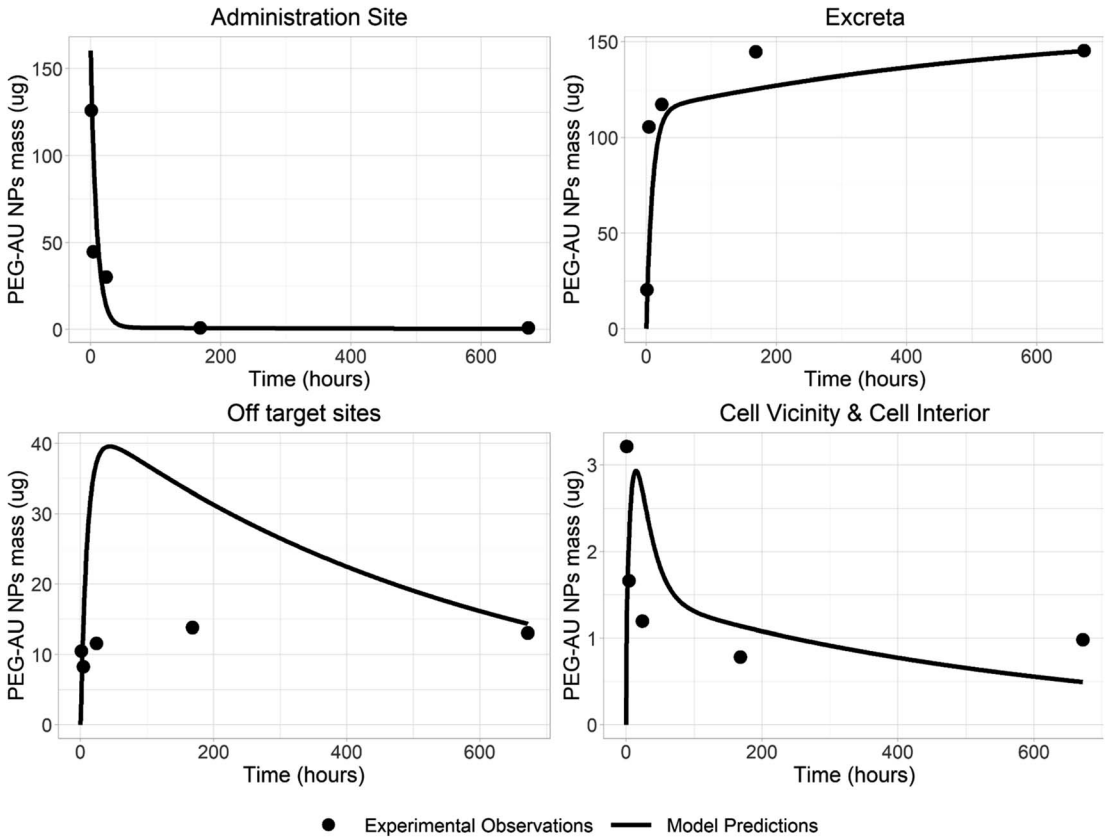

Fig. 2 Goodness-of-fit plots of the extended compartmental model for NP targeted delivery on the PEG-coated AuNPs (10 nm core size) experimental data of Kozics *et al.*[19]

influencing the delivery process. As observed in Fig. 3, the impact of reducing certain parameters is more profound in changing the resulting delivery efficiency profile compared to the impact of increasing others. Specifically, the model predicts that the highest increase in the area under the curve (AUC) of delivery efficiency can be achieved by reducing the rate of translocation from the administration site to excreta. One potential strategy to achieve this could involve increasing the particle size, thereby preventing NPs from passing through the glomerular filtration barrier due to their larger size. Another option for increasing delivery efficiency is reducing the rate of translocation from the target cell vicinity to off-target sites. However, this approach would not yield a long-lasting effect, but a rather temporary one. Therefore, simple compartmental modelling can reveal the most influential translocation parameters and indicate the direction of change – whether an increase or decrease – that is necessary to achieve optimal delivery efficiency. However, translating these findings into a design problem, specifically determining which physicochemical properties should be modified and how, remains a challenging task due to the complex interplay between NP physicochemical properties and their impact on the various translocation rates. For example, an increase in the NP's hydrodynamic size would reduce the excretion rate, but it would also inevitably influence all other translocation rates in complex ways that cannot be easily predicted or accounted for.

The R code used to acquire predictions from the extended compartmental model as well as the code for running sensitivity analysis on the model can be found at the following link: **https://github.com/ntua-unit-of-control-and-informatics/NP-delivery-modelling**.

3.3. NP delivery web application

In the context of the CompSafeNano Cloud platform, we developed a web application that leverages the extended compartmental model for describing the dynamics of NP delivery to the target cell interior. The web application integrates the presented equations into a user-friendly interface, enabling researchers and practitioners to simulate and analyze diverse scenarios related to NP-mediated *in vivo* drug delivery. By providing a comprehensive mathematical description of *in vivo* NP delivery, this web application software aims to accelerate the development of next-generation therapeutic strategies, ultimately contributing to the advancement of precision medicine and improved patient outcomes. The application is freely accessible through the following link:

https://www.enaloscloud.novamechanics.com/compsafenano/ivpd/

The web application allows users to test various 'what-if' scenarios by adjusting kinetic parameter values. By exploring these scenarios, users can observe how changes in translocation rates affect the resulting biodistribution, as reflected in the

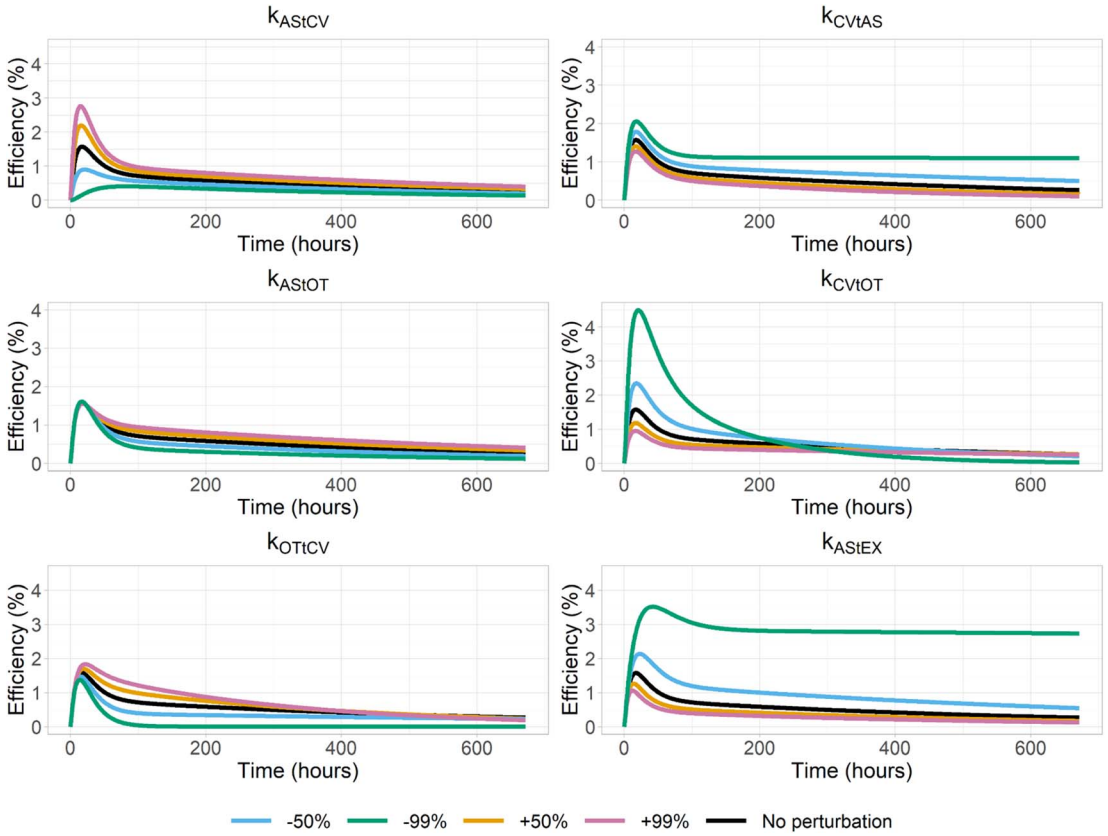

Fig. 3 Delivery efficiency for different perturbation levels in the translocation rates of the compartmental model.

generated mass–time profiles. The graphical user interface (GUI) is divided into two main sections. The first section allows users to input specific values for the model parameters. The parameters are categorized into four groups: five initial values for the state variables of the ODE system, twelve translocation rates among compartments, four degradation rates, and two simulation parameters (the integration time step and the duration of the simulation). After entering the parameter values, users can click the "Calculate Drug Delivery" button to initiate the analysis. This action generates two detailed plots. The first plot displays the evolution of the state variables of the ODE system over time. This includes tracking the total NP mass, as well as the NP mass distributed across the five compartments: the administration site, the vicinity of cells, the cell interior, off-target sites, and excreta. The second plot illustrates the temporal evolution of delivery efficiency, providing insights into how effectively the NPs are delivered to the target site over time. These visualizations help users understand the dynamic behavior of the NP distribution and efficiency of delivery based on the input parameters. An overview of the NP delivery web application is presented in Fig. 4.

Upon launching the web application, the GUI loads a preset parameterization that replicates the PEG–Au NP delivery to the lungs scenario from the demonstration case (Table 2), providing guidance for users (Fig. 4). In the demonstration case, sensitivity analysis revealed that the NP delivery efficiency to the lung tissue can only be increased by decreasing two parameters: the translocation rate from the administration site to excreta, and the translocation rate from the cell vicinity to off-target sites. Fig. 5 and 6 illustrate the impact of reducing the translocation rate from the administration site to excreta by a factor of ten, and the translocation rate from the cell vicinity to off-target sites by a similar factor, respectively. The simulations demonstrate a significant increase in NP delivery efficiency. Specifically, reducing the translocation rate from the cell vicinity to off-target sites appears to be more effective. However, the efficiency reaches a peak not observed when reducing the administration site to excreta translocation rate. Additionally, Fig. 7 shows the effect of introducing a biodegradation rate of 0.2 h^{-1} in all biological compartments except excreta. Here, the total NP mass decreases exponentially, resulting in a bell-shaped delivery efficiency profile characterised by an early maximum followed by a sharp decline. Note that this scenario serves only demonstration purposes, since AuNPs are not generally known to be biodegradable, although more recently a potential cellular biotransformation pathway has been elucidated.[28]

To obtain parameter estimates for various scenarios, including different NPs, end-users can utilize the code available at **https://github.com/ntua-unit-of-control-and-informatics/NP-delivery-modelling**. By following the instructions outlined in the README.md file, users can easily run the R scripts with minimal effort. The only required input is an appropriately formatted Excel file containing the necessary data. The code

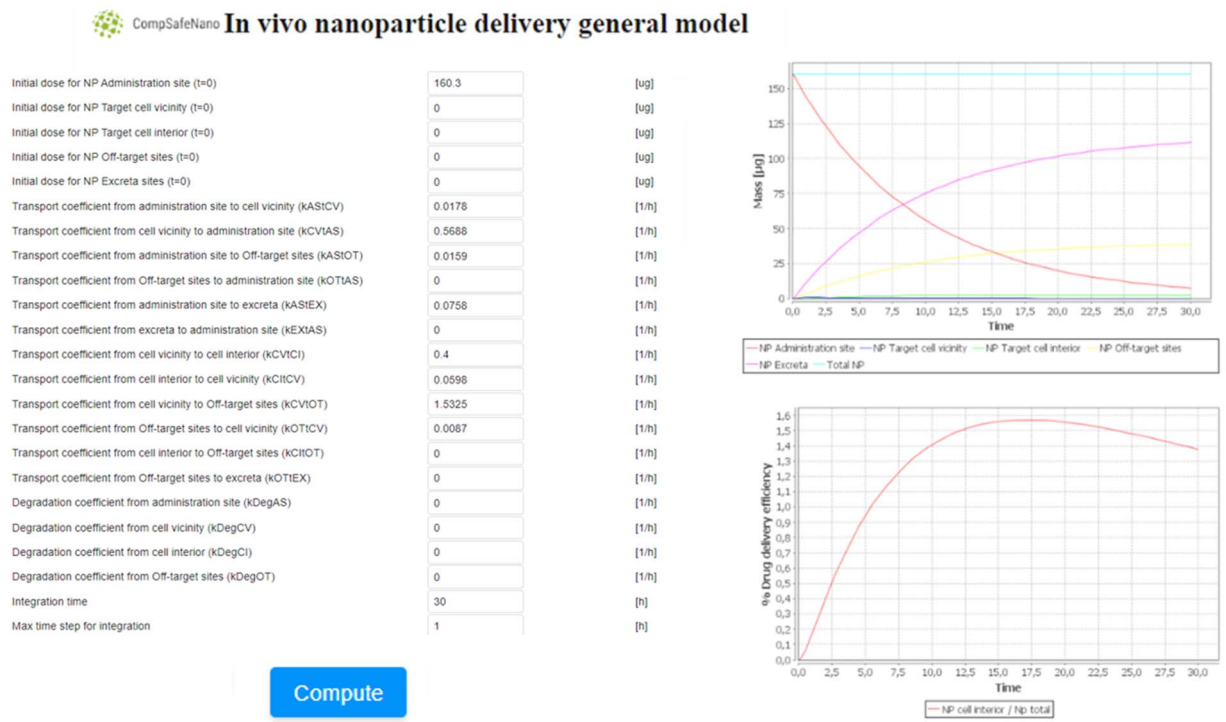

Fig. 4 Overview of the NP delivery web application, showing the input parameters on the left-hand side and the two plots generated based on solving the differential equations to show the evolution of the state variables of the ODE system over time (top right) and the temporal evolution of delivery efficiency (bottom right).

automatically fits the model to the provided data, generates parameter estimates, and produces plots for local sensitivity analysis.

The NP delivery web application is integrated into the Enalos Cloud Platform, a comprehensive suite of predictive models provided as web services (Fig. 8). This integration enhances the utility of the NP delivery model. The Enalos Cloud Platform is a freely accessible online resource in cheminformatics and nanoinformatics, offering user-friendly GUIs for a suite of nanoinformatics modeling tools. This integration lowers the barriers for conducting complex scientific computations by eliminating the need for programming skills. It supports advanced data analysis and modeling across various scientific fields, including Safe and Sustainable by Design (SSbD), making it accessible to a broader audience.

To further enhance the accessibility and integration of the NP-mediated drug delivery application, we have developed a representational state transfer (REST) application programming interface (API), accessible at **https://enaloscloud.novamechanics.com/compsafenano/swagger-ui/index.html** (Fig. 9). The implementation of the REST API is a significant contribution to this work, as it enables integration of the computational workflow into various systems and platforms. Researchers and developers can now interact with the model programmatically, without requiring direct access to the original computational environment or graphical user interface.

3.4. Data management

The complete biodistribution dataset involved in the demonstration case was cleaned, structured and uploaded into the

Fig. 5 Evaluation of the effect of reducing the translocation rate of the PEG-coated AuNPs from the administration site to excreta ten-fold on the resulting biodistribution and NP delivery efficiency.

Fig. 6 Evaluation of the effect of reducing the translocation rate of the PEG-coated AuNPs from the cell vicinity to off-target sites ten-fold on the resulting biodistribution and NP delivery efficiency.

NanoPharos database (**https://db.nanopharos.eu/**), which was developed within the Horizon 2020 (H2020) projects NanoCommons (**https://www.nanocommons.eu/**) and NanoSolveIT.[29] The NanoPharos platform follows the FAIR (Findable, Accessible, Interoperable, Reusable) data principles to provide users with high-quality, publicly accessible datasets, ready for modeling applications. It can be accessed through a REST API and is designed to readily interact with external databases. The dataset used for the parameterization of the model was thoroughly reviewed, organized, and formatted. The data have been uploaded on the NanoPharos database under the ID np28.

4. Discussion

The use of compartmental modeling constitutes a strategy for analyzing available experimental data and enables estimation of the NP delivery efficiency profile at the target site. In this work, we utilized the conceptual model proposed by ref. 18 and, for the first time, applied it to real-world data, demonstrating its practical applicability and validating its utility in a practical context. Initially, we attempted to apply the original conceptual model, which assumed irreversible NP translocation between compartments, to the demonstration case data. However, the model produced poor fits based on the generated goodness-of-fit metrics. To address this, the model was extended to include reversible kinetics, enhancing its flexibility and accuracy. As part of this extension, an additional compartment termed "excreta", was introduced. This compartment reflects the unidirectional nature of NP elimination from the body, where NPs exiting cannot re-enter. Consequently, only irreversible translocation to the excreta compartment was considered. Furthermore, NP biodegradation was incorporated into the model's general structural framework, acknowledging its potential as a critical process influencing NP biodistribution.[30,31]

The extended compartmental model represents a valuable tool for optimizing NP properties to enhance targeting and delivery. As a simple mathematical framework, it serves as an effective screening tool for comparing NPs with different characteristics *via* model fitting and parameter estimation, illustrating how variations in physicochemical properties influence NP biodistribution. Through local sensitivity analysis, we demonstrated how modeling can identify critical translocation parameters, supporting and guiding subsequent iterations in the functional-by-design framework. However, translating these *in silico* findings into tangible outcomes through NP modifications is far from straightforward. Numerous studies have explored how specific physicochemical properties of NPs influence cellular uptake and clearance mechanisms.[31–33] Yet, altering a single NP property does not solely impact a single model parameter; instead, it affects multiple parameters in interconnected and often unpredictable ways. This complex parameter interplay poses a significant challenge to the design process, complicating efforts to achieve desired outcomes.

Processing biokinetic data through simple ODE systems is concise, computationally straightforward, and cost-effective for gaining insights into delivery effectiveness. However, the model's simplicity inherently simplifies complex transport phenomena. The proposed ODE system is linear, which may

Fig. 7 Evaluation of the effect of NP biodegradation on the resulting biodistribution and NP delivery efficiency.

Fig. 8 Overview of the CompSafeNano instance within the Enalos Cloud Platform, showcasing integrated services such as the *in vivo* nanoparticle delivery general model and UANanoDock for nanoinformatics and cheminformatics modelling, enhancing accessibility to predictive tools for researchers in various scientific fields (accessed on 21 October 2024).

limit its ability to describe non-linear kinetics, such as multiphasic elimination, potentially resulting in reduced goodness-of-fit when calibrating the model against experimental data.

An alternative to the proposed strategy is mechanistic modeling, with PBK models being a prime example. These models aim to capture the complexities of physiology by introducing multiple interconnected compartments. However, this detailed structure requires the estimation of significantly more parameters. Specifically, a common approach for developing PBK models for humans involves first constructing a rodent model, which is then extrapolated to humans. Developing a PBK model for rodents requires extensive tissue sampling over time, making it both time-consuming and expensive, particularly when the goal is to optimize delivery efficiency. In contrast, the

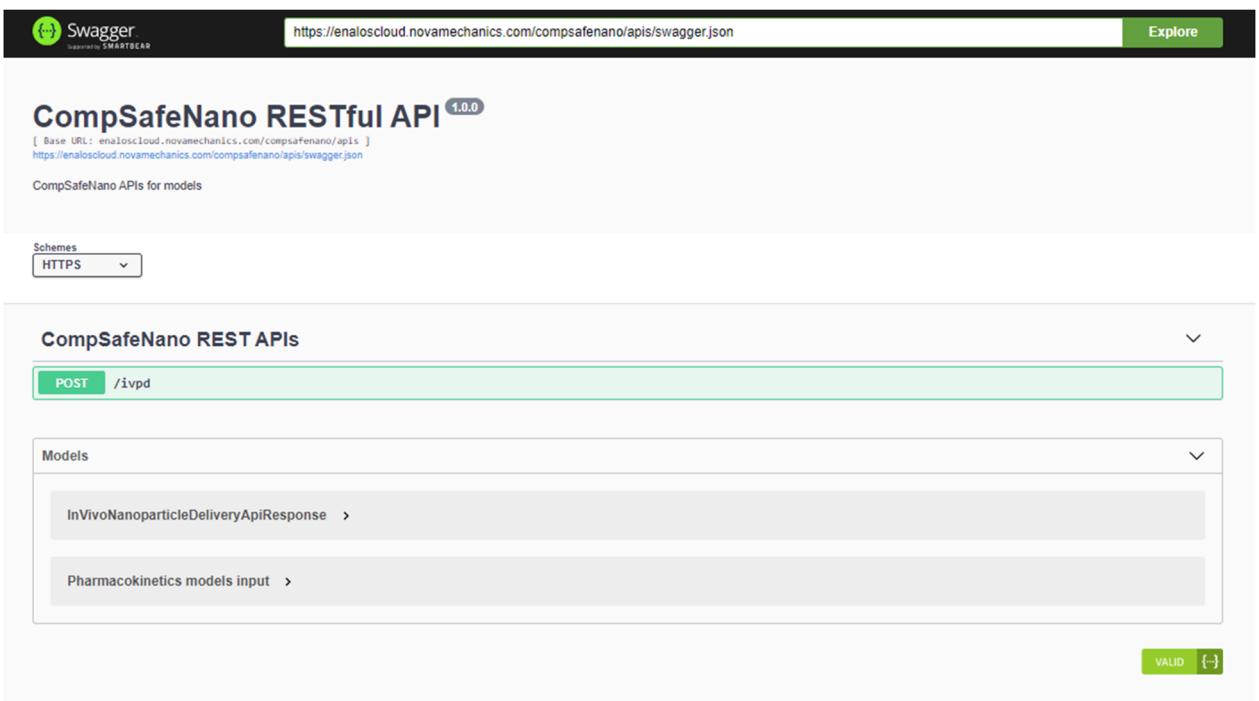

Fig. 9 The REST API environment of the model (accessed on 21 October 2024).

proposed simplified compartmental model requires minimal measurements, focusing solely on the site of interest while lumping the rest of the body into a single compartment. This approach offers a more sustainable option for screening experiments. However, the compartmental modeling approach has intrinsic limitations, as it does not support extrapolation to different scenarios, such as varying doses or species, due to its reliance on abstract kinetic parameters and lack of system-specific information. On the other hand, PBK models excel in such extrapolation tasks and, importantly, can incorporate the variability of physiological and biochemical parameters, enabling stochastic analyses of NP delivery to the target site.[34–36]

The physicochemical properties of engineered NPs vary widely, influencing their biodistribution patterns in the body after administration. Variations in characteristics such as size, surface area, shape, composition, and zeta potential significantly impact cellular uptake and the overall dynamic internal disposition.[37–39] To maintain consistency, we selected a case where both *in vivo* and *in vitro* data were available for the same NP from a single research group. Specifically, endocytosis and exocytosis rates were derived from an *in vitro* assay, while the remaining parameters were estimated using *in vivo* data. The use of cellular uptake data from *in vitro* assays to simulate *in vivo* systems has been successfully demonstrated for NPs.[21,40] However, extrapolating *in vitro* parameters to *in vivo* contexts remains challenging due to differences between the two systems that affect ADME processes, such as variations in protein content.[41] Consequently, the success and methodology of *in vitro–in vivo* extrapolation (IVIVE) are case-specific and depend heavily on both the material studied and the cell line used. An added complexity in the case of NPs is the formation of a protein corona, a dynamic *in vivo* phenomenon that strongly influences biodistribution.[42–44] Another potential limitation of this study is the reliance on rat data as a surrogate for human data. Differences in physiological and pharmacokinetic behaviors, such as immune system activity, organ perfusion, and reticuloendothelial system responses, may result in different biodistribution outcomes in humans in relation to rodents. However, the primary objective was to demonstrate how a simple compartmental model can identify major kinetic bottlenecks in NP delivery rather than serve as a predictive model. Human biodistribution data are scarce due to ethical constraints and the invasive nature of sampling. Nonetheless, a few studies have utilized imaging techniques to quantify NP biodistribution in humans.[45] In this context, rodent studies provide a more feasible approach and are widely used as proxies to generate human-relevant insights.

5. Conclusions

This study demonstrates the utility of compartmental modeling in optimizing NPs design for NP-mediated drug delivery. Compartmental modeling constitutes a robust framework for simulating and analyzing the biodistribution and delivery efficiency of NPs *in vivo*. By integrating comprehensive biological processes and incorporating reversible transport rates, the model enhances our understanding of the dynamics of NP delivery, thereby offering a valuable tool for supporting the development of targeted drug delivery strategies. The inclusion of additional compartments and reversible transport processes, as well as the consideration of NP degradation and excretion, has enabled a more detailed and accurate representation of NP behavior within the body, which can be applied for screening purposes and for analyzing the impacts of changing specific translocation rates between the compartments on NP delivery efficacy. The utility of the model was showcased through a demonstration case study involving PEG-coated Au NPs that validated the model's capacity to describe observed biodistribution patterns and provided insights into the critical parameters affecting delivery efficiency. Notably, the ability to perform sensitivity analysis has highlighted key factors, such as the impact of reducing excretion rates for example by adjusting particle size, which can improve NP delivery efficiency.

Despite the inherent limitations of compartmental models, such as their reduced predictive ability for extrapolating to different scenarios, the simplicity and computational efficiency of this approach make it a practical and valuable tool for initial assessments and hypothesis generation in NP-mediated drug delivery and development of NPs that are functional-by-design in addition to safe-by-design. The availability of the model both as a web application and as a RESTful API significantly enhances its accessibility and utility, allowing researchers to easily integrate it into their own computational workflows, automate simulations, and perform high-throughput analyses. The web application facilitates easy access to this modeling framework, empowering researchers and practitioners to explore a variety of therapeutic scenarios and optimize delivery strategies for improved patient outcomes *via* a set of "what if" scenario generation steps. Overall, this study highlights the potential of using compartmental modeling to accelerate the development of next-generation nanomedicine, contributing to the advancement of precision medicine and the realization of more effective and personalized therapeutic interventions. Future research could explore application of the model to NPs with diverse physicochemical characteristics to identify patterns and correlations. Specifically, parameter estimates could be systematically associated with specific NP properties, offering insights into how variations in size, shape, surface charge, or composition (*i.e,* different nanoforms) influence biodistribution. Another promising direction involves integrating mechanistic models in a modular fashion, particularly by replacing the target cell module. This approach could enhance parameter interpretability while preserving the overall simplicity and utility of the compartmental modeling framework.

Abbreviations

AAFE	Absolute average fold error
API	Application programming interface
AS	Administration site
AUC	Area under the curve
CI	Cell interior

CV	Cell vicinity
ENPs	Engineered nanoparticles
GUI	Graphical user interface
IVIVE	*In vitro–in vivo* extrapolation
NPs	Nanoparticles
ODE	Ordinary differential equation
OT	Off-target sites
PBK	Physiologically-based kinetic
PBPK	Physiologically-based pharmacokinetic
PEG	Polyethylene glycol
RES	Reticuloendothelial system
REST	Representational state transfer
SaaS	Software as a service
SSbD	Safe and sustainable by design
SODI	Simulations-observations discrepancy index

Data availability

Data used for the parameterization of the model for this article, including their description are available at the NanoPharos database at **https://db.nanopharos.eu/**.

Conflicts of interest

There is no competing interest among the authors.

Acknowledgements

This research was funded by the European Union's H2020 Marie Skłodowska-Curie Actions *via* CompSafeNano under (grant agreement no. 101008099).

References

1 X. Shan, X. Gong, J. Li, J. Wen, Y. Li and Z. Zhang, Current approaches of nanomedicines in the market and various stage of clinical translation, *Acta Pharm. Sin. B*, 2022, **12**, 3028–3048, DOI: **10.1016/j.apsb.2022.02.025**.

2 M. Ferrari, Cancer nanotechnology: opportunities and challenges, *Nat. Rev. Cancer*, 2005, **5**, 161–171, DOI: **10.1038/nrc1566**.

3 D. Peer, J. M. Karp, S. Hong, O. C. Farokhzad, R. Margalit and R. Langer, Nanocarriers as an emerging platform for cancer therapy, *Nat. Nanotechnol.*, 2007, **2**, 751–760, DOI: **10.1038/nnano.2007.387**.

4 R. K. Jain and T. Stylianopoulos, Delivering nanomedicine to solid tumors, *Nat. Rev. Clin. Oncol.*, 2010, **7**, 653–664, DOI: **10.1038/nrclinonc.2010.139**.

5 M. E. Davis, Z. G. Chen and D. M. Shin, Nanoparticle therapeutics: an emerging treatment modality for cancer, *Nat. Rev. Drug Discovery*, 2008, **7**, 771–782, DOI: **10.1038/nrd2614**.

6 J. M. Metselaar and T. Lammers, Challenges in nanomedicine clinical translation, *Drug Delivery Transl. Res.*, 2020, **10**, 721–725, DOI: **10.1007/s13346-020-00740-5**.

7 L. Brannon-Peppas and J. O. Blanchette, Nanoparticle and targeted systems for cancer therapy, *Adv. Drug Delivery Rev.*, 2004, **56**, 1649–1659, DOI: **10.1016/j.addr.2004.02.014**.

8 A. Z. Wang, R. Langer and O. C. Farokhzad, Nanoparticle delivery of cancer drugs, *Annu. Rev. Med.*, 2012, **63**, 185–198, DOI: **10.1146/annurev-med-040210-162544**.

9 F. Alexis, E. Pridgen, L. K. Molnar and O. C. Farokhzad, Factors affecting the clearance and biodistribution of polymeric nanoparticles, *Mol. Pharm.*, 2008, **5**, 505–515, DOI: **10.1021/mp800051m**.

10 G. Sahay, D. Y. Alakhova and A. V. Kabanov, Endocytosis of nanomedicines, *J. Controlled Release*, 2010, **145**, 182–195, DOI: **10.1016/j.jconrel.2010.01.036**.

11 E. Mahon, A. Salvati, F. Baldelli Bombelli, I. Lynch and K. A. Dawson, Designing the nanoparticle-biomolecule interface for "targeting and therapeutic delivery.", *J. Controlled Release*, 2012, **161**, 164–174, DOI: **10.1016/j.jconrel.2012.04.009**.

12 A. Nel, T. Xia, L. Mädler and N. Li, Toxic potential of materials at the nanolevel, *Science*, 2006, **311**, 622–627, DOI: **10.1126/science.1114397**.

13 V. Mirshafiee, W. Jiang, B. Sun, X. Wang and T. Xia, Facilitating Translational Nanomedicine via Predictive Safety Assessment, *Mol. Ther.*, 2017, **25**, 1522–1530, DOI: **10.1016/j.ymthe.2017.03.011**.

14 I. M. Rietjens, J. Louisse and A. Punt, Tutorial on physiologically based kinetic modeling in molecular nutrition and food research, *Mol. Nutr. Food Res.*, 2011, **55**, 941–956, DOI: **10.1002/mnfr.201000655**.

15 A. Rescigno, Compartmental analysis and its manifold applications to pharmacokinetics, *AAPS J.*, 2010, **12**, 61–72, DOI: **10.1208/s12248-009-9160-x**.

16 J. L. Y. Wu, B. P. Stordy, L. N. M. Nguyen, C. P. Deutschman and W. C. W. Chan, A proposed mathematical description of in vivo nanoparticle delivery, *Adv. Drug Delivery Rev.*, 2022, **189**, 114520, DOI: **10.1016/j.addr.2022.114520**.

17 J. Liu, Y. Y. Liu, C. S. Li, A. Cao and H. Wang, Exocytosis of Nanoparticles: A Comprehensive Review, *Nanomaterials*, 2023, **13**, 2215, DOI: **10.3390/nano13152215**.

18 J. L. Y. Wu, B. P. Stordy, L. N. M. Nguyen, C. P. Deutschman and W. C. W. Chan, A proposed mathematical description of in vivo nanoparticle delivery, *Adv. Drug Delivery Rev.*, 2022, **189**, 114520, DOI: **10.1016/j.addr.2022.114520**.

19 K. Kozics, M. Sramkova, K. Kopecka, P. Begerova, A. Manova, Z. Krivosikova, *et al.*, Pharmacokinetics, Biodistribution, and Biosafety of PEGylated Gold Nanoparticles In Vivo, *Nanomaterials*, 2021, **11**, 1702, DOI: **10.3390/nano11071702**.

20 J. Lipka, M. Semmler-Behnke, R. A. Sperling, A. Wenk, S. Takenaka, C. Schleh, *et al.*, Biodistribution of PEG-modified gold nanoparticles following intratracheal instillation and intravenous injection, *Biomaterials*, 2010, **31**, 6574–6581, DOI: **10.1016/j.biomaterials.2010.05.009**.

21 T. Dubaj, K. Kozics, M. Sramkova, A. Manova, N. G. Bastús, O. H. Moriones, *et al.*, Pharmacokinetics of PEGylated Gold Nanoparticles: In vitro-In vivo Correlation, *Nanomaterials*, 2022, **12**, 511, DOI: **10.3390/nano12030511**.

22 P. Tsiros, V. Minadakis, D. Li and H. Sarimveis, Parameter grouping and Co-estimation in physiologically-based kinetic models using genetic algorithms, *Toxicol. Sci.*, 2024, kfae051, DOI: 10.1093/toxsci/kfae051.
23 T. Rowan, *Functional Stability Analysis of Numerical Algorithms*, University of Texas at Austin, 1990.
24 K. Soetaert, T. Petzoldt and R. W. Setzer, Solving differential equations in R: package deSolve, *J. Stat. Softw.*, 2010, **33**, 1–25, DOI: 10.18637/jss.v033.i09.
25 S. G. Johnson, *nlopt*, 2024.
26 H. S. Choi, W. Liu, P. Misra, E. Tanaka, J. P. Zimmer, I. B. Itty, *et al.*, Renal clearance of quantum dots, *Nat. Biotechnol.*, 2007, **25**, 1165–1170, DOI: 10.1038/nbt1340.
27 S. Mosleh-Shirazi, M. Abbasi, M. Shafiee, S. R. Kasaee and A. M. Amani, Renal clearable nanoparticles: an expanding horizon for improving biomedical imaging and cancer therapy, *Mater. Today Commun.*, 2021, **26**, 102064, DOI: 10.1016/j.mtcomm.2021.102064.
28 A. Balfourier, N. Luciani, G. Wang, G. Lelong, O. Ersen, A. Khelfa, *et al.*, Unexpected intracellular biodegradation and recrystallization of gold nanoparticles, *Proc. Natl. Acad. Sci. U. S. A.*, 2020, **117**, 103–113, DOI: 10.1073/pnas.1911734116.
29 A. Afantitis, G. Melagraki, P. Isigonis, A. Tsoumanis, D. D. Varsou, E. Valsami-Jones, *et al.*, NanoSolveIT project: driving nanoinformatics research to develop innovative and integrated tools for in silico nanosafety assessment, *Comput. Struct. Biotechnol. J.*, 2020, **18**, 583–602, DOI: 10.1016/j.csbj.2020.02.023.
30 I. I. Vlasova, A. A. Kapralov, Z. P. Michael, S. C. Burkert, M. R. Shurin, A. Star, *et al.*, Enzymatic oxidative biodegradation of nanoparticles: mechanisms, significance and applications, *Toxicol. Appl. Pharmacol.*, 2016, **299**, 58–69, DOI: 10.1016/j.taap.2016.01.002.
31 Y. Wei, L. Quan, C. Zhou and Q. Zhan, Factors relating to the biodistribution & clearance of nanoparticles & their effects on in vivo application, *Nanomedicine*, 2018, **13**, 1495–1512, DOI: 10.2217/nnm-2018-0040.
32 J. Bourquin, A. Milosevic, D. Hauser, R. Lehner, F. Blank, A. Petri-Fink, *et al.*, Biodistribution, Clearance, and Long-Term Fate of Clinically Relevant Nanomaterials, *Adv. Mater.*, 2018, **30**, e1704307, DOI: 10.1002/adma.201704307.
33 D. Manzanares and V. Ceña, Endocytosis: The Nanoparticle and Submicron Nanocompounds Gateway into the Cell, *Pharmaceutics*, 2020, **12**, 371, DOI: 10.3390/pharmaceutics12040371.
34 J. M. Gearhart, D. A. Mahle, R. J. Greene, C. S. Seckel, C. D. Flemming, J. W. Fisher, *et al.*, Variability of physiologically based pharmacokinetic (PBPK) model parameters and their effects on PBPK model predictions in a risk assessment for perchloroethylene (PCE), *Toxicol. Lett.*, 1993, **68**, 131–144, DOI: 10.1016/0378-4274(93)90126-i.
35 P. S. Price, R. B. Conolly, C. F. Chaisson, E. A. Gross, J. S. Young, E. T. Mathis, *et al.*, Modeling interindividual variation in physiological factors used in PBPK models of humans, *Crit. Rev. Toxicol.*, 2003, **33**, 469–503.
36 F. Y. Bois, M. Jamei and H. J. Clewell, PBPK modelling of inter-individual variability in the pharmacokinetics of environmental chemicals, *Toxicology*, 2010, **278**, 256–267, DOI: 10.1016/j.tox.2010.06.007.
37 N. Oh and J. H. Park, Endocytosis and exocytosis of nanoparticles in mammalian cells, *Int. J. Nanomed.*, 2014, **9**(suppl. 1), 51–63, DOI: 10.2147/IJN.S26592.
38 M. de Almeida, E. Susnik, B. Drasler, P. Taladriz-Blanco, A. Petri-Fink and B. Rothen-Rutishauser, Understanding nanoparticle endocytosis to improve targeting strategies in nanomedicine, *Chem. Soc. Rev.*, 2021, **50**, 5397–5434, DOI: 10.1039/d0cs01127d.
39 V. Yagublu, A. Karimova, J. Hajibabazadeh, C. Reissfelder, M. Muradov, S. Bellucci, *et al.*, Overview of Physicochemical Properties of Nanoparticles as Drug Carriers for Targeted Cancer Therapy, *J. Funct. Biomater.*, 2022, **13**, 196, DOI: 10.3390/jfb13040196.
40 E. Price and A. J. Gesquiere, Animal simulations facilitate smart drug design through prediction of nanomaterial transport to individual tissue cells, *Sci. Adv.*, 2020, **6**, eaax2642, DOI: 10.1126/sciadv.aax2642.
41 E. A. Algharably, E. Di Consiglio, E. Testai, F. Pistollato, H. Mielke and U. Gundert-Remy, In Vitro-In Vivo Extrapolation by Physiologically Based Kinetic Modeling: Experience With Three Case Studies and Lessons Learned, *Front. Toxicol.*, 2022, **4**, 885843, DOI: 10.3389/ftox.2022.885843.
42 D. Dell'Orco, M. Lundqvist, C. Oslakovic, T. Cedervall and S. Linse, Modeling the time evolution of the nanoparticle-protein corona in a body fluid, *PLoS One*, 2010, **5**, e10949, DOI: 10.1371/journal.pone.0010949.
43 F. D. Sahneh, C. M. Scoglio, N. A. Monteiro-Riviere and J. E. Riviere, Predicting the impact of biocorona formation kinetics on interspecies extrapolations of nanoparticle biodistribution modeling, *Nanomedicine*, 2015, **10**, 25–33, DOI: 10.2217/nnm.14.60.
44 N. Bertrand, P. Grenier, M. Mahmoudi, E. M. Lima, E. A. Appel, F. Dormont, *et al.*, Mechanistic understanding of in vivo protein corona formation on polymeric nanoparticles and impact on pharmacokinetics, *Nat. Commun.*, 2017, **8**, 777, DOI: 10.1038/s41467-017-00600-w.
45 A. R. Péry, C. Brochot, P. H. Hoet, A. Nemmar and F. Y. Bois, Development of a physiologically based kinetic model for 99m-technetium-labelled carbon nanoparticles inhaled by humans, *Inhalation Toxicol.*, 2009, **21**, 1099–1107, DOI: 10.3109/08958370902748542.